Spatial Warping of DWI Data
Using Sparse Representation

Pew-Thian Yap and Dinggang Shen

Department of Radiology and Biomedical Research Imaging Center (BRIC)
The University of North Carolina at Chapel Hill, U.S.A
{ptyap,dgshen}@med.unc.edu

Abstract. Registration of DWI data, unlike scalar image data, is complicated by the need of reorientation algorithms for keeping the orientation architecture of each voxel aligned with the rest of the image. This paper presents an algorithm for effective and efficient warping and reconstruction of diffusion-weighted imaging (DWI) signals for the purpose of spatial transformation. The key idea is to decompose the DWI signal profile, a function defined on a unit sphere, into a series of weighted fiber basis functions (FBFs), reorient these FBFs independently based on the local affine transformation, and then recompose the reoriented FBFs to obtain the final transformed DWI signal profile. We enforce a sparsity constraint on the weights of the FBFs during the decomposition to reflect the fact that the DWI signal profile typically gains its information from a limited number of fiber populations. A non-negative constraint is further imposed so that noise-induced negative lobes in the profile can be avoided. The proposed framework also explicitly models the isotropic component of the diffusion signals to avoid undesirable reorientation artifacts in signal reconstruction. In contrast to existing methods, the current algorithm is executed directly in the DWI signal space, thus allowing any diffusion models to be fitted to the data after transformation.

1 Introduction

Spatial normalization of diffusion-weighted (DW) images often requires more than performing spatial mapping between image domains. The diffusion profile (the diffusion signals represented as a spherical function) encapsulated by each image voxel often has to be transformed to correctly align local fiber orientations. For the case of diffusion tensor imaging (DTI), this task is reduced to the reorientation of the diffusion profile based on the principal diffusion direction. For the case of high angular resolution diffusion imaging (HARDI), where the preservation of fiber crossing information is essential, the problem becomes more complicated, since the transformation has to now cater to multiple local fiber orientations in each voxel due to the existence of multiple fiber populations.

For this purpose, a decent reorientation framework was proposed by Raffelt et al. [6]. In their framework, the fiber ODF [8] is decomposed into a series of weighted spherical-harmonics-based point spread functions (PSFs), which are then reoriented individually and recomposed to form the reoriented fiber ODF. This approach was later extended in [1] for direct reorientation in the Q-space. It is further demonstrated in [1] that it is important

to take into account the isotropic component in modeling the diffusion to avoid the danger of turning an isotropic diffusion-attenuated signal profile to an anisotropic profile.

This paper proposes an algorithm for direct reorientation of the diffusion-attenuated signal profile in the Q-space by using a sparse representation framework with the DWI signal profile modeled as a combination of Watson distribution functions [10]. The proposed algorithm:

1. Avoids the computation complexity of spherical harmonics, especially that required by the associate Legendre polynomials. Although it can be argued that the spherical harmonics can be computed once and stored for subsequent computations, this strategy is generally not applicable to the case of registration, where very often the basis functions have to be computed a significant number of times, with respect to transformations that cannot be known *a priori*, as the registration algorithm iterates to refine correspondence matching;
2. Avoids the smoothing nature of spherical harmonics. When spherical harmonic basis functions of insufficient order are used, loss of sharp directional information occurs;
3. Explicitly models the isotopic diffusion component so that the isotropic content of the signal profile will not be reoriented; and
4. Incorporates an efficient non-negative L1-regularized least-squares solver, which is guaranteed to converge to the global solution in a finite number of iterative steps. This will allow us to obtain a sparse representation of the signal profile, reflecting the fact that the DWI signals at each voxel are essentially generated by a limited number of fiber populations. This is not explicitly considered in [1,6].

While employing sparse representation for diffusion modeling has been well documented (see [4] for an excellent example), the application of such framework to DWI reorientation has not been sufficiently studied. We will demonstrate that using such sparse representation framework will allow one to naturally deal with all voxels, irrespective of whether they are isotropic or highly anisotropic.

2 Approach

The proposed algorithm entails first decomposing the DWI signal profile into a series of fiber basis functions (FBFs) that are based on the Watson distribution function [10]. Given a local affine transformation, which can be computed from the local Jacobian of a deformation field estimated by any deformable registration algorithms, the FBFs are then reoriented independently and recomposed to obtain the final orientation-corrected DWI profile.

2.1 Fiber Basis Functions (FBFs)

The core of our algorithm lies in the effective decomposition of the DWI signal profile into a combination of FBFs. For better understanding of the present work, we first consider the single tensor model, with which ellipsoidal, planar and
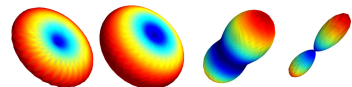
Fig. 1. The Watson distribution functions for $\kappa = -5, -1, 1, 5$

spherical directional functions can be reasonably approximated. A diffusion tensor $\mathbf{D}$ can be decomposed as $\mathbf{D} = \mathbf{U}\mathbf{K}\mathbf{U}^{\mathrm{T}}$, where $\mathbf{U}$ is a rotation matrix and $\mathbf{K}$ is a diagonal matrix of eigenvalues $\{\lambda_1, \lambda_2, \lambda_3\}$. The eigenvalues determine the shape of the tensor. For principal diffusion along a particular direction $\boldsymbol{\mu}$ (i.e., the ellipsoidal case, $\lambda_1 \gg \lambda_2 = \lambda_3$), one can approximate the exponent in the diffusion tensor model $S(\hat{\mathbf{g}}) = S_0 \exp(-b\hat{\mathbf{g}}^{\mathrm{T}}\mathbf{D}\hat{\mathbf{g}})$ as $-b\hat{\mathbf{g}}^{\mathrm{T}}\mathbf{D}\hat{\mathbf{g}} \approx -b\lambda_1\hat{\mathbf{g}}^{\mathrm{T}}(\boldsymbol{\mu}\boldsymbol{\mu}^{\mathrm{T}})\hat{\mathbf{g}} = -b\lambda_1(\boldsymbol{\mu}^{\mathrm{T}}\hat{\mathbf{g}})^2$. Thus, we have the approximation $S(\hat{\mathbf{g}}) \approx S_0 \exp(-b\lambda_1(\boldsymbol{\mu}^{\mathrm{T}}\hat{\mathbf{g}})^2)$. This equation takes a form that is identical to the probability distribution function (PDF) of the bipolar Watson distribution [10]:

$$f(\hat{\mathbf{g}}|\boldsymbol{\mu}, \kappa) = C(\kappa) \exp(\kappa(\boldsymbol{\mu}^{\mathrm{T}}\hat{\mathbf{g}})^2). \tag{1}$$

The Watson distribution function hence has tensor-like properties and is especially suited for modeling the diffusion profile. The parameter $\boldsymbol{\mu}$ is a unit vector called the *mean orientation* and κ is a constant called the *concentration parameter*. $C(\kappa)$ is a normalizing constant to ensure that the density function integrates to unity over the unit sphere. Here we note that the concentration parameter κ can take both positive and negative values, giving very different shapes for the PDF. As shown in Fig. 1, negative κ values result in donut-shaped function, which is typically the shape of the diffusion profile of a fiber population with one dominant orientation. Based on this important observation, the upcoming subsections will detail how the DWI signal profile can be decomposed into a series of FBFs of different orientations for achieving the purpose of orientation correction.

2.2 Decomposing the Diffusion-Attenuated Signal Profile

Denoting the diffusion signals measured in direction $\hat{\mathbf{g}}_i$ ($i = 1, \ldots, M$) by $S(\hat{\mathbf{g}}_i)$, our aim is to represent this spherical function based on a FBF series, which in our case is realized by a combination of Watson distribution functions:

$$S(\hat{\mathbf{g}}_i) = w_0 f_0 + \sum_{j=1}^{N} w_j f(\hat{\mathbf{g}}_i|\boldsymbol{\mu}_j, \kappa) \tag{2}$$

where $\kappa < 0$ and w_j are the weights for the FBFs $f(\cdot)$. $f_0 = C(0)$ is a constant term representing the isotropic diffusion component. The directions of the FBFs, $\boldsymbol{\mu}_j$, can be set to distribute uniformly on a sphere. In matrix form, the above equation can be rewritten as $\mathbf{S} = \mathbf{F}\mathbf{w}$, where

$$\mathbf{S} = \begin{bmatrix} S(\hat{\mathbf{g}}_1) \\ S(\hat{\mathbf{g}}_2) \\ \vdots \\ S(\hat{\mathbf{g}}_M) \end{bmatrix}, \ \mathbf{w} = \begin{bmatrix} w_0 \\ w_1 \\ \vdots \\ w_N \end{bmatrix}, \ \mathbf{F} = \begin{bmatrix} f_0 & f(\hat{\mathbf{g}}_1|\boldsymbol{\mu}_1, \kappa) & \cdots & f(\hat{\mathbf{g}}_1|\boldsymbol{\mu}_N, \kappa) \\ \vdots & \vdots & \ddots & \vdots \\ f_0 & f(\hat{\mathbf{g}}_M|\boldsymbol{\mu}_1, \kappa) & \cdots & f(\hat{\mathbf{g}}_M|\boldsymbol{\mu}_N, \kappa) \end{bmatrix}. \tag{3}$$

Assuming $M < N + 1$, we have a set of underdetermined linear equations, solution to which involves solving a least L2-norm problem:

$$\min_{\mathbf{w}} ||\mathbf{w}||_2 \text{ s.t. } \mathbf{F}\mathbf{w} = \mathbf{S}, \tag{4}$$

where $|| \cdot ||_p$ denotes the p-norm. However, to better harness the fact the DWI signals at each voxel is due to the response from a limited number of fiber populations, we compute the solution to (2) by means of a non-negative L1-regularized least-squares problem:

$$\min_{\mathbf{w}} \left\{ ||\mathbf{S} - \mathbf{Fw}||_2^2 + \beta ||\mathbf{w}||_1 \right\} \text{ s.t. } \mathbf{w} \geq \mathbf{0} \tag{5}$$

where $\beta \geq 0$ is a tuning parameter. The above problem can be solved using an active-set-based algorithm that is modified from the feature-sign algorithm presented in [5] to incorporate the non-negative constraint. The algorithm can be proven to always converge to the global optimum in a finite number of iterations.

Sparse Representation and the Isotropic Term. Determining the weight for the isotropic term by solving the least-norm problem (4) can be ambiguous. When the FBFs are distributed dense enough uniformly on a sphere, giving equal weights to all FBFs can result in an isotropic diffusion profile, hence defeating the purpose of including an isotropic term in (2) in modeling the signal profile. The sparse representation problem (5) helps avoid this pitfall by choosing the sparsest representation. In particular, in the case of an isotropic profile only w_0 will have a nonzero value.

### 2.3 Transformation and Recomposition

For signal profile correction in relation to spatial normalization, the directions of the FBFs, $\boldsymbol{\mu}_j$, are reoriented independently based on the local affine transformation matrix $\mathbf{A}$, i.e., $\boldsymbol{\mu}'_j = \frac{\mathbf{A}\boldsymbol{\mu}_j}{||\mathbf{A}\boldsymbol{\mu}_j||}$. Based on the reoriented FBFs, a new matrix in replacement of $\mathbf{F}$ can be computed as

$$\mathbf{F}' = \begin{bmatrix} f_0 & f(\hat{\mathbf{g}}_1 | \boldsymbol{\mu}'_1, \kappa) & \cdots & f(\hat{\mathbf{g}}_1 | \boldsymbol{\mu}'_N, \kappa) \\ \vdots & \vdots & \ddots & \vdots \\ f_0 & f(\hat{\mathbf{g}}_M | \boldsymbol{\mu}'_1, \kappa) & \cdots & f(\hat{\mathbf{g}}_M | \boldsymbol{\mu}'_N, \kappa) \end{bmatrix}. \tag{6}$$

The transformed DWI signal profile $\mathbf{S}'$ is finally obtained as $\mathbf{S}' = \mathbf{F}'\mathbf{w}$. Note that the isotropic component is not reoriented.

3 Experimental Results

We will first describe how the ODF and the orientations of the ODF peaks can be computed for the purpose of evaluation. We will then describe our evaluation based on simulated and *in vivo* data. For all experiments, we set $\beta = M/N$ and $\kappa = -\kappa' = -b\lambda_1$. For the *in vivo* data, λ_1 was estimated from the corpus callosum. A total of 501 orientations generated by optimizing the covering algorithm (see [2]) were used as the mean orientations of the FBFs. $T = 1281$ orientations [2] were used to locate the ODF peaks.
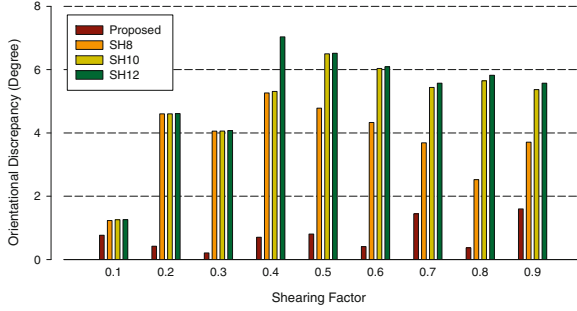
Fig. 2. Orientational discrepancy of the fiber orientations detected after reorientation with respect to the ground truth orientations
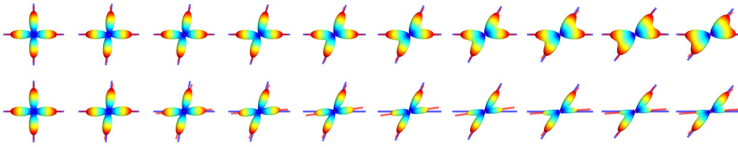

Fig. 3. Estimated fiber orientations after profile reorientation for the proposed method (top) and SH8 (bottom). Red: estimated orientations; Blue: ground truth orientations. The results from left to right correspond to shearing factor $\alpha = 0.0, 0.1, \ldots, 0.9$.

3.1   Computing the ODF and the ODF Peaks

The ODF associated with a Watson distribution function can be written as [7] $\mathcal{O}[f(\hat{\mathbf{g}}_i|\boldsymbol{\mu}_j, \kappa)] \propto f(\hat{\mathbf{g}}_i|\boldsymbol{\mu}_j, \kappa')$ with $\kappa' > 0$. We can hence write $\mathcal{O}[S(\hat{\mathbf{g}}_i)] = w_0 f_0 + \sum_j^N w_j f(\hat{\mathbf{g}}_i|\boldsymbol{\mu}_j, \kappa')$. A concentration $\kappa' = -\kappa/2$ will give results similar to that derived in [7], which is based on the method suggested by Tuch [9]. A larger value of κ' will give results closer to the sharper fiber ODF [8]. For simplicity, we used $\kappa' = -\kappa$ for all experiments. To extract the orientations of the ODF peaks, which represent the local fiber orientations, the following steps were performed:

1. Sample the ODF with sufficient density at orientations $\hat{\mathbf{w}}_1, \ldots \hat{\mathbf{w}}_T$.
2. Remove orientations associated with ODF values less than the mean value.
3. Locate orientations with values greater than their neighboring orientations.
4. Compute the mean orientations of the orientations in the neighborhood of the orientations with the maximal values. This can be done by computing the eigenvector corresponding to the largest eigenvalue of the dyadic tensor $\mathbf{D}_{\text{dyadic}}(\hat{\mathbf{w}}_i) = \frac{1}{|\mathcal{N}(\hat{\mathbf{w}}_i)|} \sum_{\mathbf{v} \in \mathcal{N}(\hat{\mathbf{w}}_i)} \mathbf{v}\mathbf{v}^{\mathrm{T}}$ for $\hat{\mathbf{w}}_i$ satisfying $\mathcal{O}[S(\hat{\mathbf{w}}_i)] > \mathcal{O}[S(\mathbf{v})], \forall \mathbf{v} \in \mathcal{N}(\hat{\mathbf{w}}_i)$. $\mathcal{N}(\hat{\mathbf{w}}_i)$ denotes the neighborhood of $\hat{\mathbf{w}}_i$. Return the mean orientations as the output.
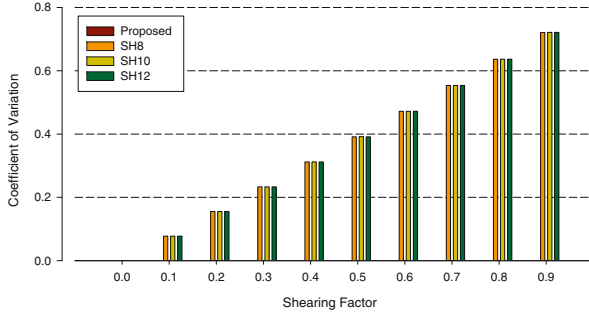
Fig. 4. Preservation of isotropy after reorientation. A greater c.v. value indicates higher anisotropy. Note that the values given by the proposed method is consistently zero for all cases; therefore, they are not visible.
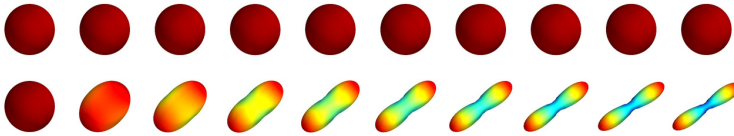
Fig. 5. Reorientation results for the proposed method (top) and SH8 (bottom) using shearing factor $\alpha = 0.0, 0.1, \ldots, 0.9$. With the proposed method, the isotropy of the profile is faithfully preserved.

3.2   Simulated Data

Assuming 2 crossing fiber populations, we used a mixture of diffusion tensors to generate a diffusion profile representing a fiber crossing for the evaluation of the proposed method. Each fiber population is represented by a tensor with $\lambda_1 = 5 \times 10^{-3} \text{mm}^2/\text{s}$, $\lambda_2 = \lambda_3 = 5 \times 10^{-4} \text{mm}^2/\text{s}$ and $b = 1000 \text{s}/\text{mm}^2$. The (120) gradient directions were taken from the *in vivo* dataset. One tensor is oriented in the horizontal (x-axis) direction and the other in the vertical (y-axis) direction.

Reorientation Accuracy. The diffusion profile was sheared in the horizontal direction using the transformation matrix $\mathbf{A} = [1 \; \alpha \; 0; \; 0 \; 1 \; 0; \; 0 \; 0 \; 1]$, where α is the *shearing factor*, increment of which will result in a greater degree of shearing. We set $\alpha = 0.1, 0.2, \ldots, 0.9$. The ground-truth orientations were computed by reorienting directly the orientations of the individual tensors, i.e., $[1, 0, 0]$ and $[0, 1, 0]$. We evaluated the accuracy of the reorientated diffusion profile by comparing fiber orientations detected from it with respect to the ground truth. Assuming that $\mathbf{U}$ is the set of ground truth orientations and $\mathbf{V}$ is the corresponding set of estimated orientations, the *orientational discrepency* is defined as $\frac{1}{2} \left[\frac{1}{|\mathbf{U}|} \sum_{\mathbf{u} \in \mathbf{U}} \min_{\mathbf{v} \in \mathbf{V}} d_\theta(\mathbf{u}, \mathbf{v}) + \frac{1}{|\mathbf{V}|} \sum_{\mathbf{v} \in \mathbf{V}} \min_{\mathbf{u} \in \mathbf{U}} d_\theta(\mathbf{v}, \mathbf{u}) \right]$, where $d_\theta(\mathbf{u}, \mathbf{v})$ gives the angle difference between $\mathbf{u}$ and $\mathbf{v}$, i.e., $d_\theta(\mathbf{u}, \mathbf{v}) = \cos^{-1}(|\mathbf{u} \cdot \mathbf{v}|)$. The absolute value is taken since diffusion is assumed to be antipodal symmetric.

The results are shown quantitatively in Fig. 2 and qualitatively in Fig. 3. The results generated using Raffelt et al.'s method [6], applied directly to the ODF using spherical harmonics up to order 8 (SH8), 10 (SH10), and 12 (SH12), are also included for comparison. Note that for the proposed algorithm the ODFs were computed based on the reoriented DWI signal profiles, whereas for the comparison method reorientation was performed directly on the ODF. The results indicate that the proposed method 1) yields lesser error in the estimated orientations, and 2) affects less the diffusion profile in the horizontal direction, which is to be expected, since shearing is applied in the horizontal direction.
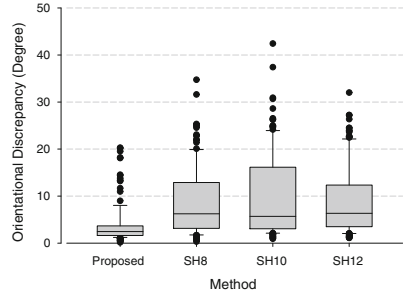

Fig. 6. Reorientation accuracy evaluated using *in vivo* data

Preservation of Isotropy. We also evaluated the proposed method on whether it can successfully preserve the isotropy of an isotropic profile. For this purpose, we measured the anisotropy of the reoriented ODFs using the coefficient of variation c.v. $= \frac{\text{std}(\mathcal{O}[\mathbf{S}])}{\langle\mathcal{O}[\mathbf{S}]\rangle}$, recalling that $\mathcal{O}[\cdot]$ is the ODF operator previously defined. A larger c.v. value indicates a greater degree of anisotropy.

We generated an isotropic diffusion profile with constant signal magnitude $\exp(-b\lambda)$, where $b = 1000\text{s/mm}^2$ and $\lambda = 5 \times 10^{-3}\text{mm}^2/\text{s}$, in all directions. This profile was then subject to the different degree of shearing identical to the experiment using simulated data. The c.v. values of the reoriented ODFs were then measured as an indication of whether the reorientation algorithm unnecessarily distorts the originally isotropic profile. The results, shown in Fig. 4, demonstrate the importance of explicitly modeling the isotropic diffusion component. Neglecting this will cause the originally isotropic profile to become anisotropic after reorientation, which cannot be physically true. Visual results for comparison are shown in Fig. 5, where it can be seen that the distortion for the representative case of SH8 is quite apparent.

3.3   Real Data

Diffusion-weighted images were acquired for an adult subject using a Siemens 3T TIM Trio MR Scanner with an EPI sequence. Diffusion gradients were applied in 120 non-collinear directions with diffusion weighting $b = 2000\text{s/mm}^2$. The imaging matrix was 128×128 with a rectangular FOV of $256 \times 256\text{mm}^2$. 80 contiguous slices with a slice thickness of 2mm covered the whole brain.

We extracted DWI signal profiles from the voxels located in the pons, since this location of the brain was found to contain a significant amount of fiber crossings [3]. The profiles were randomly transformed using the matrix $\mathbf{A} = [1\ \alpha\ 0;\ 0\ 1\ 0;\ 0\ 0\ 1]\,\mathbf{R}$, where $\mathbf{R} = \mathbf{R}_x\mathbf{R}_y\mathbf{R}_z$ is composed by matrices of rotations around the x, y, and z axes. The local orientations prior to profile reorientation were estimated and transformed using the corresponding matrix $\mathbf{A}$ to serve as ground truth for evaluation of the

reorientation algorithms. The reorientation accuracy was measured by computing the orientational discrepancy of the estimated orientations with respect to the ground truth. The results, shown in Fig. 6, again confirms that the proposed method yields markedly improved results.

4   Conclusion

We have presented in this paper a novel algorithm for the transformation of raw DWI data directly in the Q-space. The algorithm takes into account of the isotropic diffusion component and can therefore be applied to any voxels without requiring explicitly masking out gray matter and cerebospinal fluid voxels. The capability of working directly with the diffusion signal profiles implies that the transformed outcome will allow the plethora of diffusion models to be fitted after the fact. It is not difficult to envision that future works involving registration, segmentation, and voxel-based analysis using diffusion-weighted images will benefit fundamentally from the current work.

References

 1. Dhollander, T., Van Hecke, W., Maes, F., Sunaert, S., Suetens, P.: Spatial transformations of high angular resolution diffusion imaging data in Q-space. In: Workshop on Computational Diffusion MRI (CDMRI), Medical Image Computing and Computer Assisted Intervention (MICCAI), pp. 73–83 (2010)
 2. Hardin, R.H., Sloane, N.J.A., Smith, W.D.: Tables of spherical codes with icosahedral symmetry, http://www2.research.att.com/~njas/icosahedral.codes/
 3. Jeurissen, B., Leemans, A., Tournier, J.D., Jones, D.K., Sijbers, J.: Estimating the number of fiber orientations in diffusion MRI voxels: a constrained spherical deconvolution study. In: ISMRM 2010 (2010)
 4. Jian, B., Vemuri, B.C.: A unified computational framework for deconvolution to reconstruct multiple fibers from diffusion weighted MRI. IEEE Transactions on Medical Imaging 26(11), 1464–1471 (2007)
 5. Lee, H., Battle, A., Raina, R., Ng, A.Y.: Efficient sparse coding algorithms. In: NIPS, pp. 801–808 (2007)
 6. Raffelt, D., Tournier, J.D., Fripp, J., Crozier, S., Connelly, A., Salvado, O.: Non-linear spatial normalisation of high angular resolution diffusion imaging data using fiber orientation distributions. In: Workshop on Diffusion Modelling and the Fibre Cup (DMFC), Medical Image Computing and Computer Assisted Intervention (MICCAI), pp. 73–83 (2009)
 7. Rathi, Y., Michailovich, O., Shenton, M.E., Bouix, S.: Directional functions for orientation distribution estimation. Medical Image Analysis 13(3), 432–444 (2009)
 8. Tournier, J.D., Calamante, F., Gadian, D.G., Connelly, A.: Direct estimation of the fiber orientation density function from diffusion-weighted MRI data using spherical deconvolution. NeuroImage 23(3), 1176–1185 (2004)
 9. Tuch, D.: Q-ball imaging. Magnetic Resonance in Medicine 52(6), 1358–1372 (2004)
10. Watson, G.: Equatorial distributions on a sphere. Biometrika 52, 193–201 (1965)